

Suppression of Mn photoluminescence in ferromagnetic state of Mn-doped ZnS nanocrystals

I. Sarkar,¹ M. K. Sanyal,¹ S. Takeyama,² S. Kar,³ H. Hirayama,² H. Mino,⁴ F. Komori,² and S. Biswas³

¹Surface Physics Division, Saha Institute of Nuclear Physics, Kolkata 700 064, India

²Institute for Solid State Physics, University of Tokyo, Chiba 277-8581, Japan

³Department of Material Science, Indian Association for the Cultivation of Science, Kolkata 700032, India

⁴Graduate School of Science and Technology, Chiba University, Chiba 263-8522, Japan

(Received 3 September 2008; revised manuscript received 13 November 2008; published 11 February 2009)

Magnetic ordering can tune optical properties of photoluminescent dilute magnetic semiconductors. The results of a magnetic field dependent photoluminescence (PL) up to 50 T above and below ferromagnetic transition temperature T_C in Mn-doped ZnS nanocrystals have been reported here. The PL intensity corresponding to internal transition between states of Mn significantly decreases with application of magnetic field below T_C but no such suppression was observed above T_C even at 50 T. The zero-field PL intensity also exhibits continuous suppression with decreasing temperature in the ferromagnetic state. The PL intensity profiles could be fitted consistently using a model of magnetic-ordering-induced spin-sensitive energy transfer to Mn states below T_C .

DOI: [10.1103/PhysRevB.79.054410](https://doi.org/10.1103/PhysRevB.79.054410)

PACS number(s): 75.75.+a, 71.35.Ji, 71.55.Gs, 75.50.Pp

I. INTRODUCTION

Nanoparticles of dilute magnetic semiconductors (DMSs) have been an active field of research for their exotic optical as well as magnetic properties that can lead to wide range of possible optoelectronic applications.¹ In II-VI DMS, manganese (Mn)-doped zinc sulfide (ZnS) forms a very important system because of its efficient luminescent properties.² Numerous studies have been focused on Mn-doped ZnS nanoparticles as the d -electron states of Mn is known to be an efficient luminescent center³ that can activate photoluminescence (PL). Recently, Mn-doped ZnS nanoparticles (~ 2.5 nm) were found to order ferromagnetically around 30 K.⁴ Confinement-induced ferromagnetic ordering in these systems has also been investigated theoretically through first-principles calculations and ferromagnetic ordering has been obtained for nanocrystal having less than 3 nm size.⁵ This is expected to bring forth new vistas to the optical studies of these materials. Several studies have been reported on excitonic⁶⁻¹¹ and some on internal Mn-PL intensity^{12,13} as functions of magnetic field and temperature.¹⁴⁻¹⁶ However, while the $sp-d$ exchange interaction is known to lead to magnetic ordering in DMS,^{4,5,17} no studies to the best of our knowledge have been reported that show effect of magnetic ordering on internal Mn-PL emission. The study of excitonic complexes with magnetic polarons for wideband DMS nanostructures such as ZnS is hindered in time-resolved magnetoluminescence¹⁸ as the PL spectrum is dominated by internal $Mn^{2+} 3d^5$ luminescence band with a peak around 590 nm (2.1 eV). A study of magnetic field dependence of Mn PL over a large range can give a method to probe various excitonic complexes that may be formed below T_C , in particular for DMS nanostructures and also in general for DMS.

Here we report on magnetic field dependence of Mn-PL spectra below and above ferromagnetic ordering temperature T_C in nanocrystals of Mn-doped ZnS. The measurements were carried out to a very high magnetic field of 50 T. The results obtained in these measurements could be explained with a model (elaborated in the Appendix) that invokes spin-

dependent restriction of energy transfer between exciton and Mn^{2+} states. Here we also report on the effect of magnetic ordering on thermal dependence of internal Mn-PL intensity of Mn-doped ZnS nanoparticles. Formation of various kinds of exciton magnetic polaron (EXMP) complexes is expected to play an important role in PL processes observed in DMS. The thermal dependence or stability of EXMP can be given by¹⁹ free-energy difference of EXMP and free exciton that varies as²⁰

$$F(T) = T \ln \left[\cosh \left(\frac{\Delta}{K_B T} \right) \right], \quad (1)$$

where Δ is the spin splitting energy for carriers.

The Mn-doped ZnS nanocrystallites were found to be ferromagnetic below 30 K [Fig. 1(a)], marked by branching in ZFC-FC magnetization, hysteresis and giant Zeeman splitting in spin-PLE data.⁴ Here we present experimental results that show decrease in the PL intensity of the internal Mn transition with application of magnetic field only in ordered state below the ferromagnetic transition temperature T_C [Fig. 1(b)]. The zero-field PL intensity below T_C also decreased with decreasing temperature. The result was interpreted by a simple model in which the spin-dependent energy transfer from excitons to Mn ions is restricted by the ferromagnetic ordering of Mn spins. However no suppression of Mn PL was observed for 1.5% Mn concentration Zn(Mn)S nanocrystals that do not exhibit [Fig. 1(c)] ferromagnetic order and associated ZFC-FC branching and giant Zeeman splitting.⁴

The importance of the internal Mn transitions stems from the fact that the PL spectrum of Mn-doped ZnS is dominated by internal $Mn^{2+} 3d^5$ luminescence band with a peak around 590 nm (2.1 eV) accompanied by quenching of excitonic emission in the band-gap region of ZnS because of efficient energy transfer to Mn system. The internal Mn transition occurs between the first excited state 4T_1 and the ground state 6A_1 of $3d^5$ shell of Mn having spin states of 3/2 and 5/2, respectively. As both of these states are composed of energy

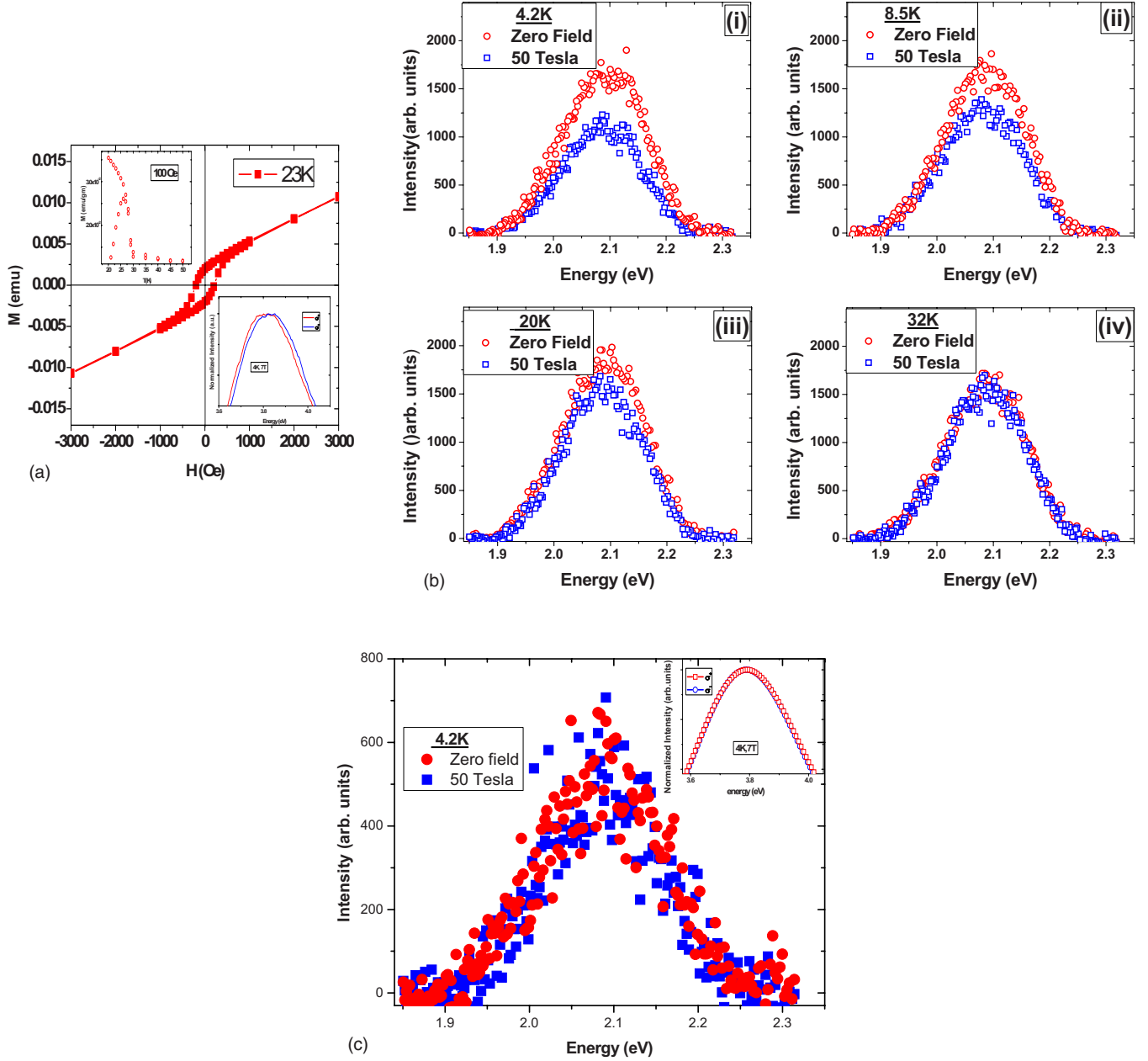


FIG. 1. (Color online) (a) The figure shows hysteresis at 23 K, branching in zero-field-cooled (ZFC) and field-cooled (FC) magnetization at 100 Oe with a sharp rise in magnetization ~ 30 K and giant Zeeman splitting in spin-polarized photoluminescence excitation (spin-PL) data at 4 K for 2.5% Mn-doped Zn(Mn)S. (b) PL spectra corresponding to transition between internal Mn^{2+} states for zero magnetic field and 50 T at varying temperatures of (i) 4.2 K, (ii) 8.5 K, (iii) 20 K, and (iv) 32 K for 2.5% Mn-doped sample. The difference in PL intensity in the presence and absence of magnetic field reduces as the temperature is increased toward T_C . (c) Mn-PL spectra for 1.5% Mn-doped Zn(Mn)S that do not order magnetically. No PL suppression is observed. The inset shows the absence of giant Zeeman splitting in this system.

levels of d^5 centers, they are of the same parity (even) states. As a result this transition is forbidden in free Mn ion as electric dipole transition is forbidden for the same parity and also for the different spin states. However substitutional doping of Mn in ZnS host nanoparticles causes strong exchange interaction due to hybridization of s - p electrons of the ZnS and d electrons of Mn.²¹ This interaction along with crystal field effects leads to relaxation of forbiddance^{22,23} that allows the yellow orange emission corresponding to internal Mn transition. Moreover this interaction in nanocrystals leads to

interesting observations²⁴ such as coexistence of multiple lifetimes^{25–27} due to confinement.

II. EXPERIMENTAL PROCEDURES

The Mn-doped ZnS nanocrystallites were prepared by a solvo-thermal technique.²⁸ The details of preparation and characterization have been reported previously.⁴ PL measurements reported here were carried out on 2.5% Mn-doped ZnS nanocrystals using a 40 ms pulsed magnet by applying a

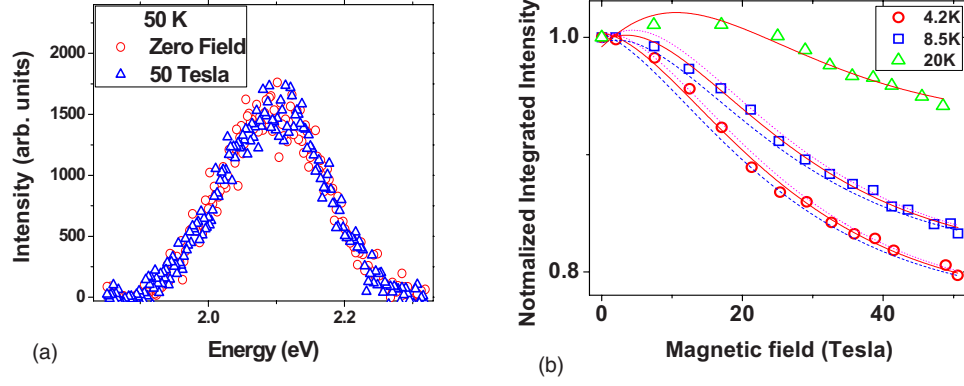


FIG. 2. (Color online) (a) Mn-PL spectra in presence and absence of magnetic field at 50 K. No field dependence is observed. (b) Magnetic field dependence of normalized integrated intensity at 4.2, 8.5, and 20 K. The normalized integrated intensity at a given temperature is obtained by integrating over the whole peak and then normalizing with respect to the zero-field integrated intensity at that temperature. The solid curve gives the fit using Eq. (4) for $g=1.12$. The dotted and dashed lines for 4.2 and 8.5 K correspond to fit for $g=1.2$ and 1, respectively.

maximum field of 50 T with 0.8 ms integration time at each field window. However the PL corresponding to excitonic emission could not be detected due to lack of intensity. The samples were excited using HeCd laser having 325 nm wavelength. PL spectrum was recorded using an image intensified charge-coupled device (CCD) camera in a streak mode. A Band-edge filter was used to cut off any possible plasma lines coming from laser or due to higher harmonics from grating in the range of measurements. Measurements were carried at varying field both below and above magnetic ordering temperature of ~ 30 K. Care was taken to arrest any possible movement of sample due to vibration produced during discharging of magnet. Spin-polarized measurements of PL were not possible because of very weak signal strength. The thermal variation of zero-field PL spectrum was recorded in a standard Oxford designed cryostat magnet by varying temperature from 4 to 65 K in the absence of magnetic field using a combination of a double monochromator and a water-cooled photomultiplier tube.

III. RESULTS AND DISCUSSIONS

The magnetic field dependence of internal Mn^{2+} PL at different temperatures [Fig. 1(b)] clearly reveals significant difference in zero-field and high-field PL spectra indicating large reduction in the intensity at low temperatures below the ordering temperature $T_C \sim 30$ K. A 20% quenching of normalized integrated PL intensity was observed at 4.2 K at 50 T [Fig. 2(b)]. However the degree of suppression of the PL intensity decreases with increasing temperature as T_C is approached. Just above T_C there is negligible difference between PL intensity in the presence and absence of magnetic field [Fig. 1(b)]. Well above T_C no suppression of PL intensity could be observed [Fig. 2(a)]. At a given temperature below T_C , PL intensity decreases as the field is increased [Fig. 2(b)]. This reflects a *strong correlation* between magnetic ordering and internal Mn-PL transition. Unlike the standard exponential suppression of Mn PL predicted¹² and observed in DMS quantum well structures,¹³ here initially the PL intensity decreases slowly and then rapidly decreases at

higher fields for 4.2 and 8.5 K. The normalized integrated intensity is obtained by integrating the intensity over the entire energy range of 1.9–2.25 eV and then normalizing with respect to the integrated intensity at zero magnetic field for each temperature.

In the presence of magnetic field the ground level 6A_1 having spin 5/2 and the first excited level with spin 3/2, namely, 4T_1 of the five d electron states of Mn split^{12,29} into six and four nondegenerate states, respectively. As the dipole selection rule requires conservation of Mn^{2+} spin state ($\Delta S_z = 0$) (Ref. 12) during the transition, the participation from of 4T_1 level to $\pm 5/2$ states of 6A_1 level gets blocked as the field is increased resulting in reduction in PL intensity. This blocking leads to exponential decay of internal Mn-PL intensity^{7,12} that can be expressed as¹³

$$I(B) \sim \exp\left(-\frac{\gamma B}{T}\right), \quad (2)$$

where B is the magnetic field and γ is a constant at a given temperature T . However this expression is not expected to explain the observed field dependence with magnetic ordering as the theory did not take full account of the total angular and spin moments of excitons and Mn.³⁰

The magnetic ordering will have direct consequences on the spin-selective energy transfer from exciton to Mn states. For II-VI DMS the spin selection rules are different for photoexcited excitonic state having $J=1$ and $J=2$ states.³⁰ The $J=1$ state obeys the model of Eq. (2) and thus one gets exponential suppression of PL with magnetic field. For $J=2$ state the selection rules for internal Mn transition requires $\Delta S_z = \pm 1$ thus even $\pm 5/2$ states of 6A_1 level can participate³⁰ and hence no PL suppression is expected for $J=2$.

The zero-field PL intensity (Fig. 3) corresponding to internal Mn transition also shows strong temperature dependence below T_C . The normalized integrated intensity in zero field is obtained by normalizing with respect to the zero-field integrated intensity at 35 K. As the temperature is reduced below T_C the zero-field PL intensity decreases (Fig. 3). How-

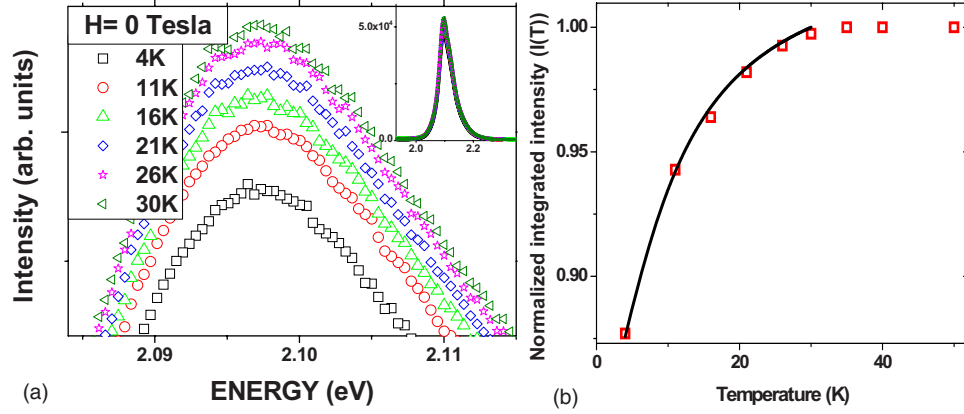


FIG. 3. (Color online) (a) Temperature dependence of Mn-PL spectra at zero magnetic field. The inset shows the PL spectrum for the whole range of measurement. (b) Temperature dependence of normalized PL intensity at zero field. The normalization is done with respect to the intensity at 35 K. The solid curve gives fit to the observed thermal dependence below T_C using Eq. (3). Above T_C no observable variation was observed in the measured range of 70 K.

ever above T_C there is no observable thermal dependence in the measured range of temperature of 70 K (Fig. 3). A 15% reduction in zero-field Mn-PL intensity is observed compared to PL intensity above 30K [Fig. 3(b)]. This further adduces to the fact that magnetic ordering affects the transfer of energy to Mn states leading to reduction in corresponding PL intensity.

The process of energy transfer to the Mn states is very complex. The internal Mn-PL behavior depends on two factors: first the efficiency of energy transfer from excitonic states to Mn states and second to the relaxation of forbidden transition between 4T_1 and 6A_1 levels (Fig. 4). A possible explanation to the observed PL intensity variation with temperature below T_C can be given using a simple model (refer to the Appendix for details) that assumes an additive contribution of nonexcitonic and excitonic complexes. The model further assumes that a fraction of excitonic complexes decay without contributing to Mn-PL intensity. As the magnetic ordering gets settled in below T_C , the photocreated excitons can get polarized by forming complexes with magnetic polaron.^{31–33} These excitons may lower their energy by forming exciton complexes such as charged EXMP or EXMP complexes that do not allow efficient transfer of energy to Mn states, hence quenching the corresponding PL intensity.

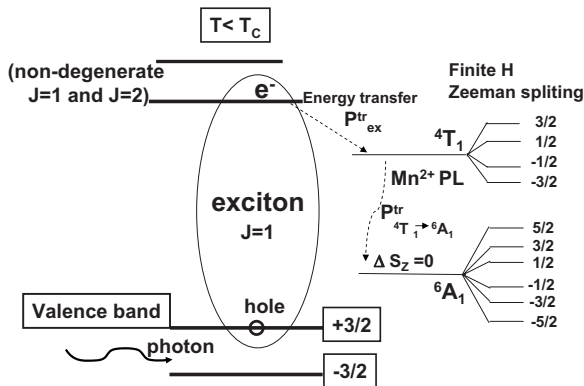


FIG. 4. The expected model for energy transfer to Mn states from an excitonic state below T_C .

Assuming a thermal dependence similar to Eq. (1) for the excitonic complexes formed below T_C , the PL intensity should reduce with $F(T)$ as $F(T)$ grows with reduction in temperature T . Hence below T_C normalized zero-field Mn-PL intensity may be modeled as

$$I_N(T) = 1 - bT \ln \left[\cosh \left(\frac{\Delta}{K_B T} \right) \right], \quad (3)$$

where b is a constant. As Δ depends on strength of internal field, so assume it to have similar thermal dependence as coercive field H_C ,⁴ it can be expressed as $\Delta = \Delta_0(1 - T/T_C)^{0.5}$. Equation (3) was found to fit the thermal dependence below T_C of the zero-field normalized integrated intensity data [Fig. 3(b)] very well, with $b = 0.0126$ and $\Delta_0 = 1.166$ meV as fitting parameters.

The magnetic field dependence of PL intensity can be understood by further considering relaxation of the forbidden transition between 4T_1 and 6A_1 levels. Below T_C the $J=1$ and $J=2$ states should become nondegenerate with $J=1$ being the more populated state as it corresponds to lower energy. Hence the magnetic ordering enforces spin-selective energy transfer as the $J=1$ state restricts the internal transition between Mn states to the requirement of no change in spin projection of Mn states during the transition (Fig. 4). These complexes then transfer energy to the Mn^{2+} levels (Fig. 4) depending on their thermal stability. This transferred energy then decays through inter-Mn²⁺ levels depending on the extent of relaxation of the forbiddance to the interlevel transition. The absence of any magnetic field dependence of PL above T_C can be explained by the destruction of magnetic ordering of these nanocrystals as the temperature is raised and T_C is approached. Thus the spin polarization reduces and finally vanishes above T_C , resulting in degeneracy of $J=1$ or $J=2$ state. Hence the forbiddance of internal Mn transition due to the restriction of $\Delta S_z = 0$ for Mn spins gets lifted by additional allowance of $\Delta S_z = \pm 1$ because of $J=2$ state.

The normalized integrated field-dependent PL intensity $N(B, T_f)$ with respect to zero-field PL at a fixed temperature T_f can be written as (refer to the Appendix)

$$N(B, T_f) = \alpha + \lambda T \ln \left[\cosh \left(\frac{\Delta + g\mu_B B}{K_B T} \right) \right] \exp \left(-\frac{\gamma B}{T} \right), \quad (4)$$

where α and λ are both constants at a fixed temperature. An excellent simultaneous fit [Fig. 2(b)] of different temperature data of field dependence of the normalized integrated PL intensity was obtained using Eq. (4) over a wide range of field up to 50 T with the same value of $\Delta_0 = 1.166$ meV (Ref. 34) obtained from the fit of thermal dependence of zero-field PL intensity using Eq. (3) [Fig. 3(b)]. The best fit was obtained for the value of $g = 1.12$ and $\lambda = 0.023(\pm 0.001)$. Figure 2(b) shows fitted lines for three values of 1, 1.12, and 1.2 for g . For similar Mn-based II-VI DMS nanocrystals g of carriers has been found to be around 1.2.⁵ For 4.2 and 8.5 K values of α are found to be 0.78 and 0.81, respectively. The small decrease in value of α with decrease in temperature is expected as $F(T)$ increases with decrease in temperature. γ for 4.2 and 8.5 K are found to be 0.29 and 0.59, respectively. The reduction in value of γ is expected for such high-field measurements as it is indicative of the strength of Mn-Mn interaction. As the temperature is lowered γ is quenched due to enhanced direct Mn-Mn antiferromagnetic interaction. This is further important in high-field measurements as, for fields above 15 T, Mn PL starts getting contributions from Mn-Mn clusters.¹² For a paramagnetic system where fields around 7 T are enough to saturate all Mn spins, γ is proportional to a constant Landé (g) factor for Mn under the assumption of single Mn ion excitations and no contribution from Mn-Mn interaction.^{12,13} The data for 20 K normalized field-dependent PL intensity show a very small rise at lower fields and then it falls off at higher field as expected from this simple model for temperatures above 15 K. However an exact fit with this simple model for a suppression of $\sim 5\%$ yields a high value of $\gamma = 1.6$ with $\alpha = 0.92$ and $\lambda = 0.038$. Such large values of γ and λ indicate that the simplified model presented here needs to be refined further. We have not attempted it here as the change in PL intensity and the kind of statistics observed here at higher temperature prohibit us to do detailed analysis. However it is interesting to note that even this simplified model reproduces initial rise at low field for the 20 K data.

Experimental results presented here clearly show a decrease in the PL intensity of the internal Mn transition with application of magnetic field below the ferromagnetic transition temperature T_C . The zero-field PL intensity below T_C also decreased with decreasing temperature. The absence of any such behavior in both zero-field and field measurements clearly established the fact that observed change is related to magnetic ordering. Furthermore no PL suppression was observed for sample that does not order magnetically. These facts established the observed PL suppression to occur due to magnetic ordering and hence ruled out the possibility of observed PL suppression due to magnetic field dependence of the absorption coefficient magnetic field due to the Zeeman effect and diamagnetic or Landau shift of the states in ZnS clusters that are excited by the laser in the given experiments.

IV. CONCLUSION

To summarize, dependence of PL intensity corresponding to internal Mn transmission in magnetically ordered Mn-doped ZnS nanoparticles has been observed. A strong suppression of PL is reported both in the presence and absence of magnetic field below ferromagnetic ordering temperature T_C . No tangible effects either of temperature or magnetic field is observed above T_C . The magnetic ordering is found to induce suppression of the efficiency of internal Mn PL. The results could be understood by invoking magnetic-ordering-induced spin-dependent restriction of energy transfer to Mn states that gets relaxed above T_C . Although the simple model presented here could explain the data, a detailed spectroscopic model will be required to explain the actual nature of the excitonic complexes formed below T_C . Furthermore the study of magnetic field dependence of Mn PL over a large range can give a method to probe various excitonic complexes that may be formed below T_C , in particular for DMS nanostructures and also in general for DMS especially in systems where the direct probe of excitonic complexes is hindered due to the presence of stronger radiative decay through internal Mn levels.

ACKNOWLEDGMENTS

I.S. would like to thank DST and Surface Interface Science (SIS) subject group of India-Japan Cooperative Science Programme (IJCSP) for supporting part of this work.

APPENDIX

The internal Mn^{2+} PL intensity may be expressed as $I(B, T) = \zeta - \chi_{\text{ex}}^{\text{dir}} + \chi_{\text{ex}}^{\text{Mn}}$, where ζ is the intensity in the nonmagnetic state above T_C when there is no contribution from excitonic complexes with magnetic polaron and is constant. $\chi_{\text{ex}}^{\text{Mn}}$ is the excitonic component related to magnetic polaron that decays through Mn states having an exponential dependence on magnetic field and $\chi_{\text{ex}}^{\text{dir}}$ is the excitonic component related to the magnetic polaron that does not decay through Mn states and increases with increasing stability of excitonic complexes, with magnetic polarons, and with lowering of temperature. However direct determination of $\chi_{\text{ex}}^{\text{dir}}$ is not possible due to its weak strength. Both the terms depend on the stability of excitonic complexes. $\chi_{\text{ex}}^{\text{dir}} = dF(T)$, where d is some constant and $F(T)$ varies as Eq. (1), as also seen in thermal dependence of zero-field Mn PL. $\chi_{\text{ex}}^{\text{Mn}} = eH(B, T)$, where e is some constant. $H(B, T)$ can be written as

$$H(B, T) = P_{\text{ex}}^{\text{tr}} P_{4T_1 \rightarrow 6A_1}^{\text{tr}}, \quad (A1)$$

where $P_{\text{ex}}^{\text{tr}}$ is the efficiency of transfer of energy from exciton to $4T_1$ and $P_{4T_1 \rightarrow 6A_1}^{\text{tr}}$ is the efficiency of inter- Mn^{2+} level transition. $P_{\text{ex}}^{\text{tr}}$ should have a thermal dependence as Eq. (1). However as the spin splitting increases with magnetic field the argument of \cosh in Eq. (1) needs to be modified as $(\Delta + g\mu_B B)/K_B T$, where B is magnetic field and g is the g factor for carriers. Field and thermal dependences of $P_{4T_1 \rightarrow 6A_1}^{\text{tr}}$ are given by Eq. (2). Thus $H(B, T)$

$=T \ln[\cosh(\frac{\Delta + g\mu_B B}{K_B T})] \exp(-\frac{\gamma B}{T})$; also, $H(B=0, T)=F(T)$. The generalized equation can thus be modeled as $I(B, T)=\zeta - dF(T) + eH(B, T)$. We can recover Eq. (3) from this generalized equation as $I_N(T)=\frac{I(0, T)}{I(0, 35 \text{ K})}=1-bF(T)$, where $b=(d-e)/\zeta$ under the assumption that, as 35 K is above ordering temperature T_C , Mn PL at this temperature is not expected to have any contribution from the excitonic complexes with magnetic polaron, making $I(0, 35 \text{ K}) \approx \zeta$. The normalized integrated field-dependent PL intensity $N(B, T_f)$ with respect to zero-field PL at a fixed temperature T_f is given by

$$N(B, T_f) = \frac{\zeta - dF(T_f) + eH(B, T_f)}{\zeta - dF(T_f) + eH(0, T_f)}. \quad (\text{A2})$$

As $H(0, T)=F(T)$,

$$N(B, T_f) = \zeta^{-1} [\zeta - dF(T_f) + eH(B, T_f)] \left[1 - \frac{(d-e)}{\zeta} F(T_f) \right]^{-1}. \quad (\text{A3})$$

Here $(d-e)/\zeta \ll 1$ as $e, d < \zeta$, as can be observed by a reduction of about 15% in zero-field PL at 4.2 K with respect to PL at 35 K and a 20% reduction at most at highest field of 50 T at 4.2 K with respect to zero-field PL at 4.2 K. $N(B, T_f)$ can be simplified as

$$N(B, T_f) = \alpha + \lambda T \ln \left[\cosh \left(\frac{\Delta + g\mu_B B}{K_B T} \right) \right] \exp \left(-\frac{\gamma B}{T} \right), \quad (\text{A4})$$

where $\alpha = [1 - (\frac{e}{\zeta} + \frac{d(d-e)}{\zeta^2}) F(T_f)]$ and $\lambda = [\frac{e}{\zeta} + \frac{e(d-e)}{\zeta^2} F(T_f)]$.

-
- ¹D. J. Norris, A. L. Efros, and S. C. Erwin, *Science* **319**, 1776 (2008).
 - ²J. W. Allen, *J. Phys. C* **19**, 6287 (1986).
 - ³R. N. Bhargava, D. Gallagher, X. Hong, and A. Nurmikko, *Phys. Rev. Lett.* **72**, 416 (1994).
 - ⁴I. Sarkar, M. K. Sanyal, S. Kar, S. Biswas, S. Banerjee, S. Chaudhuri, S. Takeyama, H. Mino, and F. Komori, *Phys. Rev. B* **75**, 224409 (2007).
 - ⁵S. J. Cheng, *Phys. Rev. B* **77**, 115310 (2008).
 - ⁶L. V. Khoi, J. Kossut, and R. R. Galazka, *J. Supercond.* **16**, 427 (2003).
 - ⁷V. G. Abramishvili, A. V. Komarov, S. M. Ryabchenko, and Y. G. Semenov, *Solid State Commun.* **78**, 1069 (1991).
 - ⁸H. Falk, W. Heimbrot, P. J. Klar, J. Hübner, M. Oestreich, and W. W. Rühle, *Phys. Status Solidi B* **229**, 781 (2002).
 - ⁹E. A. Chekhovich, A. S. Brichkin, A. V. Chernenko, V. D. Kulakovskii, I. V. Sedova, S. V. Sorokin, and S. V. Ivanov, *Phys. Rev. B* **76**, 165305 (2007).
 - ¹⁰A. Golnik, J. Ginter, and J. A. Gaj, *J. Phys. C* **16**, 6073 (1983).
 - ¹¹B. König, U. Zehnder, D. R. Yakovlev, W. Ossau, T. Gerhard, M. Keim, A. Waag, and G. Landwehr, *Phys. Rev. B* **60**, 2653 (1999).
 - ¹²M. Nawrocki, Y. G. Rubo, J. P. Lascaray, and D. Coquillat, *Phys. Rev. B* **52**, R2241 (1995).
 - ¹³S. Lee, M. Dobrowolska, and J. K. Furdyna, *Phys. Rev. B* **72**, 075320 (2005).
 - ¹⁴F. H. Su, B. S. Ma, Z. L. Fang, K. Ding, G. H. Li, and W. Chen, *J. Phys.: Condens. Matter* **14**, 12657 (2002).
 - ¹⁵M. Tanaka and Y. Masumoto, *Chem. Phys. Lett.* **324**, 249 (2000).
 - ¹⁶J. Yu, H. Liu, Y. Wang, F. E. Fernandez, and W. Jia, *J. Lumin.* **76-77**, 252 (1998).
 - ¹⁷P. Kacman, *Semicond. Sci. Technol.* **16**, R25 (2001).
 - ¹⁸J. Seufert, G. Bacher, M. Scheibner, A. Forchel, S. Lee, M. Dobrowolska, and J. K. Furdyna, *Phys. Rev. Lett.* **88**, 027402 (2001).
 - ¹⁹T. Stirner, P. Harrison, W. E. Hagston, and J. P. Goodwin, *Phys. Rev. B* **50**, 5713 (1994).
 - ²⁰M. Umehara, *Phys. Rev. B* **67**, 035201 (2003).
 - ²¹T. A. Kennedy, E. R. Glaser, P. B. Klein, and R. N. Bhargava, *Phys. Rev. B* **52**, R14356 (1995).
 - ²²K. Yan, C. Duan, Y. Ma, S. Xia, and J. C. Krupa, *Phys. Rev. B* **58**, 13585 (1998).
 - ²³N. Q. Huang and J. L. Birman, *Phys. Rev. B* **69**, 085321 (2004).
 - ²⁴L. Chen, T. Niebling, W. Heimbrot, D. Stichtenoth, C. Ronning, and P. J. Klar, *Phys. Rev. B* **76**, 115325 (2007).
 - ²⁵A. A. Bol and A. Meijerink, *Phys. Rev. B* **58**, R15997 (1998).
 - ²⁶B. A. Smith, J. Z. Zhang, A. Joly, and J. Liu, *Phys. Rev. B* **62**, 2021 (2000).
 - ²⁷L. Chen, F. J. Brieler, M. Fröba, P. J. Klar, and W. Heimbrot, *Phys. Rev. B* **75**, 241303(R) (2007).
 - ²⁸S. Biswas, S. Kar, and S. Chaudhuri, *J. Phys. Chem. B* **109**, 17526 (2005).
 - ²⁹A. Kamińska and A. Suchocki, *J. Appl. Phys.* **84**, 6753 (1998).
 - ³⁰A. V. Chernenko, P. S. Dorozhkin, V. D. Kulakovskii, A. S. Brichkin, S. V. Ivanov, and A. A. Toropov, *Phys. Rev. B* **72**, 045302 (2005).
 - ³¹G. Mackh, M. Hilpert, D. R. Yakovlev, W. Ossau, H. Heinke, T. Litz, F. Fischer, A. Waag, G. Landwehr, R. Hellmann, and E. O. Göbel, *Phys. Rev. B* **50**, 14069 (1994).
 - ³²S. Takeyama, S. Adachi, Y. Takagi, and V. F. Aguekian, *Phys. Rev. B* **51**, 4858 (1995).
 - ³³I. A. Merkulov, G. R. Pozina, D. Coquillat, N. Paganotto, J. Siviniant, J. P. Lascaray, and J. Cibert, *Phys. Rev. B* **54**, 5727 (1996).
 - ³⁴The value of zero-field spin splitting energy Δ obtained from the model [refer to Eq. (3)] for excitonic complexes formed with magnetic polarons is different from the direct giant Zeeman splitting observed at 7 T at 4.2 K in the spin-polarized PLE measurements (Ref. 4), as the spin PLE can only access the bare excitonic state before forming a polaron state (Ref. 32).